Dynamics of active droplet formation in reaction-driven Cahn-Hilliard models

EMS Topical Activity Group Mixtures, Prague 2025

A. Signori, *(Joint collaboration: H. Garcke, K.F. Lam, R. Nürnberg)*

Alexander von HUMBOLDT STIFTUNG

POLITECNICO MILANO 1863

Biological Motivation

• D. Zwicker, R. Seyboldt, C. A. Weber, A. A. Hyman, and F. Jülicher, Growth and division of active droplets provides a model for protocells. *Nature Phys.*, **3984** (2016).

Biological Motivation

A **protocell** is cell-like structure that models how the first living cells might have formed.

- **Droplets as early life models** as chemical reaction centers.
  - **Protocell model**: active droplets could model early protocells with simple metabolic processes.

• H. Garcke, K.F. Lam, R. Nürnberg and **A.S.**, On a Cahn–Hilliard equation for the growth and division of chemically active droplets modeling protocells. *Work in progress*.

◦ H. Garcke, K.F. Lam, R. Nürnberg and **A.S.**, On a Mullins–Sekerka model for the growth of active droplets modeling protocells: Stability analysis and numerical computations. *Work in progress*.

- J. Bauermann, G. Bartolucci, J. Boekhoven, C. A. Weber, and F. Jülicher, Formation of liquid shells in active droplet systems. *Phys. Review Research*, **5** (2023).
  - D. Zwicker, R. Seyboldt, C. A. Weber, A. A. Hyman, and F. Jülicher, Growth and division of active droplets provides a model for protocells. *Nature Phys.*, **3984** (2016).

Diffuse Interface Model (PF)

We consider the **diffuse interface model**

$$\begin{aligned}
\partial_t \varphi &= \operatorname{div}(m(\varphi)\nabla\mu) + S_\varepsilon(\varphi) && \text{in } Q := \Omega \times (0,T),\\
\mu &= \beta(-\varepsilon\Delta\varphi + \tfrac{1}{\varepsilon}\psi'(\varphi)) && \text{in } Q,\\
m(\varphi)\partial_{\mathrm{n}}\mu &= \partial_{\mathrm{n}}\varphi = 0 && \text{on } \Gamma := \partial\Omega \times (0,T),\\
\varphi(0) &= \varphi_0 && \text{in } \Omega,
\end{aligned}$$

with $\psi(r) = \frac{1}{4}(1-r^2)^2$. The source term $S_\varepsilon \in C^1(\mathbb{R})$ is given by

$$S_\varepsilon(\varphi) = \begin{cases} S_+ - \frac{1}{\varepsilon}K_+(\varphi - 1) & \varphi \geq 1,\\ \text{cubic interpolation} & \varphi \in (-1,1),\\ S_- - \frac{1}{\varepsilon}K_-(\varphi + 1) & \varphi \leq -1,\end{cases}$$

$S_+ < 0$, $S_- > 0$, and $K_\pm > 0$.

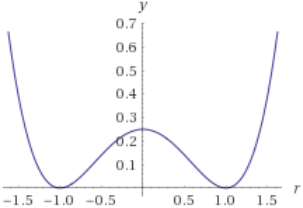

- J. W. Cahn and J. E. Hilliard. Free energy of a nonuniform system. I. interfacial free energy. *J. Chem. Phys.*, **28**(2):258–267, 1958.
- J. W. Cahn. On spinodal decomposition. *Acta metallurgica*, **9**(9):795–801, 1961.

Sharp Interface Model (SI)

We set: $\Omega^{\pm} = \Omega(t)^{\pm} := \{x \in \Omega : \varphi(x,t) = \pm 1\}$, $\Sigma(t) :=$ interface of the phases,

and $m_{\pm} := m(\pm 1)$. As $\varepsilon \to 0$, we find

$$
\begin{aligned}
-m_+ \Delta \mu &= S_+ - \rho_+ \mu && \text{in } \Omega^+, \\
-m_- \Delta \mu &= S_- - \rho_- \mu && \text{in } \Omega^-, \\
\mu &= \frac{\gamma \beta \kappa}{2} && \text{on } \Sigma, \\
[\mu]_-^+ &= 0 && \text{on } \Sigma, \\
-2\mathcal{V} &= [m \nabla \mu]_-^+ \cdot \boldsymbol{\nu} + \mathcal{S}_* && \text{on } \Sigma, \\
\partial_{\mathbf{n}} \mu &= 0 && \text{on } \partial\Omega,
\end{aligned}
$$

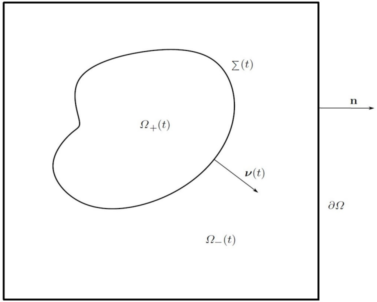

$\rho_{\pm} = \frac{K_{\pm}}{\beta \psi''(\pm 1)}$, $\gamma \in \mathbb{R}$ depending on ψ, κ mean curvature of Σ, $\mathcal{S}_* \in \mathbb{R}$ depends on S.

◦ W. W. Mullins and R. F. Sekerka: *J. Appl. Phys.* 64', *J. Appl. Phys.* 65', *J. Chem. Phys.* 85'.

Theoretical results

Theorem (Well-posedness of the PF model)

For every $\varphi_0 \in H^1$, there exists a unique weak solution (φ, μ):

$$\varphi \in H^1(0,T;(H^1)^*) \cap L^\infty(0,T;H^1) \cap L^2(0,T;H^2), \quad \mu \in L^2(0,T;H^1),$$

satisfying, for every $v \in H^1$ and almost every $t \in (0,T)$,

$$\langle \partial_t \varphi, v\rangle_{H^1} + \int_\Omega m(\varphi)\nabla\mu\cdot\nabla v = \int_\Omega S_\varepsilon(\varphi)v,$$
$$\int_\Omega \mu v = \beta\varepsilon\int_\Omega \nabla\varphi\cdot\nabla v + \frac{\beta}{\varepsilon}\int_\Omega \psi'(\varphi)v.$$

Moreover, let $\{(\varphi_i,\mu_i)\}_i$, $i=1,2$, two solutions with initial data $\varphi_{0,i}\in H^1$, $i=1,2$ and $m\equiv 1$. Then, it holds that

$$\|(\varphi_1-\varphi_2)-(\varphi_1-\varphi_2)_\Omega\|_{L^\infty(0,T;(H^1)^*)\cap L^2(0,T;H^1)} + \|(\varphi_1)_\Omega-(\varphi_2)_\Omega\|_{L^\infty(0,T)}$$
$$\leq K\big(\|(\varphi_{0,1}-(\varphi_{0,1})_\Omega)-(\varphi_{0,2}-(\varphi_{0,2})_\Omega)\|_* + |(\varphi_{0,1})_\Omega-(\varphi_{0,2})_\Omega|\big),$$

for $K>0$ just depending on structural data.

Schematic Idea of the Method

We introduce the **signed distance** function d to Σ_0 with $d > 0$ in Ω^+ and $d < 0$ in Ω^-, $\nabla d = \boldsymbol{\nu}$ and set $z = \frac{d}{\varepsilon}$. We parametrize Σ_0 by arc-length as $g(t,s)$. In a tubular neighborhood of Σ_0, a **smooth function** f is rewritten as:

$$f(x) = f(g(t,s) + \varepsilon z \boldsymbol{\nu}(g(t,s))) =: F(t,s,z).$$

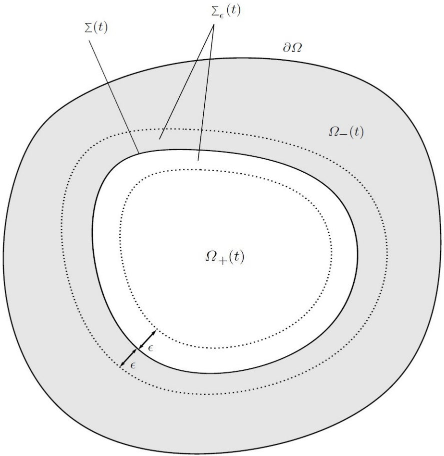

- $\partial_t f \approx -\frac{1}{\varepsilon}\mathcal{V}\partial_z F$
  - $\nabla_x f \approx \frac{1}{\varepsilon}\partial_z F \boldsymbol{\nu} + \nabla_{\Sigma_0} F$
- $\Delta_x f \approx \frac{1}{\varepsilon^2}\partial_{zz} F - \frac{1}{\varepsilon}\kappa\partial_z F$

∇_{Σ_0} is the surface gradient on Σ_0,
$\kappa = -\operatorname{div}_{\Sigma_0}\boldsymbol{\nu}$ the mean curvature.

Sharp Interface Model (SI)

$$
\begin{aligned}
-m_+\Delta\mu &= S_+ - \rho_+\mu && \text{in } \Omega^+,\\
-m_-\Delta\mu &= S_- - \rho_-\mu && \text{in } \Omega^-,\\
\mu &= \frac{\gamma\beta\kappa}{2} && \text{on } \Sigma,\\
[\mu]_-^+ &= 0 && \text{on } \Sigma,\\
-2\mathcal{V} &= [m\nabla\mu]_-^+\cdot\boldsymbol{\nu} + \mathcal{S}_* && \text{on } \Sigma,\\
\partial_{\mathrm{n}}\mu &= 0 && \text{on } \partial\Omega,
\end{aligned}
$$

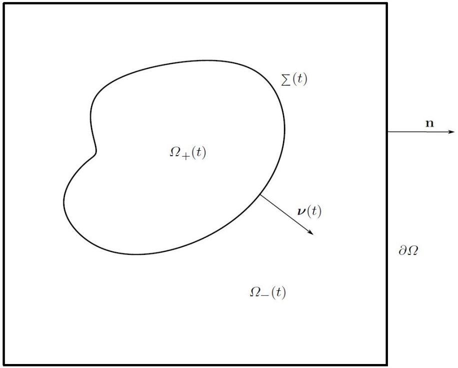

- $\rho_\pm = \frac{K_\pm}{\beta\psi''(\pm 1)}$;
  - $\gamma \in \mathbb{R}$ depending on ψ;
  - κ is the mean curvature of Σ;
- $\mathcal{S}_* \in \mathbb{R}$ depends on S.

Perturbation of Planar Solutions

Planar Solutions

We study the (SI) in:

$$\Omega = (0, \mathcal{L}) \times (0, \tilde{\mathcal{L}})^{d-1}, \quad \mathcal{L}, \tilde{\mathcal{L}} > 0,$$

and seek for a planar solution in

$$\Omega_+(t) = (0, q(t)) \times (0, \tilde{\mathcal{L}})^{d-1}, \quad \Omega_-(t) = (q(t), \mathcal{L}) \times (0, \tilde{\mathcal{L}})^{d-1},$$

where $q(t)$ encodes the location of the interface Σ_0.
We set $x = (z, \hat{x})$ with $z \in \mathbb{R}$ and $\hat{x} \in \mathbb{R}^{d-1}$. As $\boldsymbol{\nu} = (-1, 0)^\top$ we get $\mathcal{V} = -\dot{q}$ and make the ansatz

$$\mu_\pm(t, (z, \hat{x})) = \hat{\mu}_\pm(t, z), \quad z \in (0, \mathcal{L}), \hat{x} \in (0, \tilde{\mathcal{L}})^{d-1}.$$

Original System

$$\begin{aligned}
-m_+ \Delta\mu &= S_+ - \rho_+ \mu && \text{in } \Omega^+, \\
-m_- \Delta\mu &= S_- - \rho_- \mu && \text{in } \Omega^-, \\
\mu &= \tfrac{\gamma\beta\kappa}{2} && \text{on } \Sigma, \\
[\mu]_-^+ &= 0 && \text{on } \Sigma, \\
-2\mathcal{V} &= [m\nabla\mu]_-^+ \cdot \boldsymbol{\nu} + S_I && \text{on } \Sigma, \\
\partial_{\mathbf{n}}\mu &= 0 && \text{on } \partial\Omega,
\end{aligned}$$

Planar Scenario

$$\begin{aligned}
-m_+ \mu_+'' &= S_+ - \rho_+ \mu_+ && \text{for } z \in (0, q(t)), \\
-m_- \mu_-'' &= S_- - \rho_- \mu_- && \text{for } z \in (q(t), \mathcal{L}), \\
\mu_+'(t, 0) &= 0, \\
\mu_-'(t, \mathcal{L}) &= 0, \\
2\dot{q} &= -[m\mu']_-^+ + S_I.
\end{aligned}$$

We obtain as solutions

$$\mu_+(t,z) = d_+\left(1 - \frac{\cosh(\Lambda_+ z)}{\cosh(\Lambda_+ q(t))}\right), \quad \mu_-(t,z) = d_-\left(1 - \frac{\cosh(\Lambda_-(\mathcal{L}-z))}{\cosh(\Lambda_-(\mathcal{L}-q(t)))}\right),$$

where $d_\pm := \frac{S_\pm}{\rho_\pm} = \beta\frac{S_\pm \psi''(\pm 1)}{K_\pm}$, and $\Lambda_\pm := \sqrt{\frac{\rho_\pm}{m_\pm}}$. The evolution equation $2\dot{q} = -[m\mu']_-^+ + S_I$ for the interface position becomes

$$\dot{q} = \frac{1}{2}\left(d_+ m_+ \Lambda_+ \tanh(\Lambda_+ q) + d_- m_- \Lambda_- \tanh(\Lambda_-(\mathcal{L} - q)) + S_I\right) =: \mathcal{H}(q).$$

We notice that

$$\mathcal{H}(0) = \frac{1}{2}(d_- m_- \Lambda_- \tanh(\Lambda_- \mathcal{L}) + S_I), \quad \mathcal{H}(\mathcal{L}) = \frac{1}{2}(d_+ m_+ \Lambda_+ \tanh(\Lambda_+ \mathcal{L}) + S_I).$$

Claim:

The existence of a root q^* of $\mathcal{H}$ can be guaranteed.

For instance: $S_+ = -1$, all other parameters equal to 1 $\Rightarrow$ $q^* = \frac{\mathcal{L}}{2}$.

General case: after fixing parameters, one can adjust L in S_I to ensure the existence of a root.

Linear Stability of Planar Solutions

Goal: Analyse stability of planar solutions $\mu_\pm^*$ around position q^*.

We consider a perturbed interface $w := q^* + \epsilon Y$, with $Y = Y(t, \hat{x})$. We make the ansatz

$$\mu_\pm(t,x) = \mu_\pm^*(z) + \epsilon u_\pm(t,x),$$

and demand that those solve the FBP

$$\begin{aligned}
&-m_+\Delta(\mu_+^* + \epsilon u_+) = S_+ - \rho_+(\mu_+^* + \epsilon u_+) && \text{in } \{z < w\},\\
&-m_-\Delta(\mu_-^* + \epsilon u_-) = S_- - \rho_-(\mu_-^* + \epsilon u_-) && \text{in } \{z > w\},\\
&\mu_+^* + \epsilon u_+ = \mu_-^* + \epsilon u_- && \text{on } \{z = w\},\\
&2(\mu_\pm^* + \epsilon u_\pm) = \gamma\beta\kappa && \text{on } \{z = w\},\\
&-2\mathcal{V} = [m\nabla(\mu^* + \epsilon u)]_-^+ \cdot \boldsymbol{\nu} + S_I && \text{on } \{z = w\},\\
&(\mu_+^* + \epsilon u_+)'(t,0) = 0, \quad (\mu_-^* + \epsilon u_-)'(t,\mathcal{L}) = 0.
\end{aligned}$$

Linearizing the above equations around $\{z = q^*\}$, produces

$$
\begin{aligned}
&-m_+\Delta u_+ = -\rho_+ u_+ && \text{in } \{z < q^*\},\\
&-m_-\Delta u_- = -\rho_- u_- && \text{in } \{z > q^*\},\\
&(\mu_+^*)'|_{z=q^*} Y + u_+ = (\mu_-^*)'|_{z=q^*} Y + u_- && \text{on } \{z = q^*\},\\
&2((\mu_\pm^*)'|_{z=q^*} Y + u_\pm) = -\gamma\beta\Delta_{\hat{x}} Y && \text{on } \{z = q^*\},\\
&2\dot{Y} = -m_+((\mu_+^*)''|_{z=q^*} Y + u_+') + m_-((\mu_-^*)''|_{z=q^*} Y + u_-') && \text{on } \{z = q^*\},\\
&(u_+)'(t,0) = 0, \quad (u_-)'(t,\mathcal{L}) = 0.
\end{aligned}
$$

$\boxed{\text{Ansatz: } u_\pm(x) = v_\pm(z)W(\hat{x})}$ and choose W as an eigenfunction of the $\Delta_{\hat{x}}$-operator with Neumann boundary conditions such that for $\hat{\boldsymbol{\ell}} = (\ell_2, \dots, \ell_d) \in \mathbb{N}_0^{d-1}$,

$$
\begin{cases}
\Delta_{\hat{x}} W = \frac{\zeta_{\hat{\boldsymbol{\ell}},d}}{(\widetilde{\mathcal{L}})^2} W & \text{in } (0,\widetilde{\mathcal{L}})^{d-1},\\
\partial_{\mathrm{n}} W = 0 & \text{on } \partial(0,\widetilde{\mathcal{L}})^{d-1}.
\end{cases}
$$

A possible eigenfunction is

$$
W(x_2, \dots, x_d) = \cos\left(\frac{\pi}{\widetilde{\mathcal{L}}}\ell_2 x_2\right) \times \dots \times \cos\left(\frac{\pi}{\widetilde{\mathcal{L}}}\ell_d x_d\right), \quad \zeta_{\hat{\boldsymbol{\ell}},d} = -\pi^2(\ell_2^2 + \dots + \ell_d^2).
$$

With this ansatz for $u_\pm$ we find that

$$-m_\pm(v''_\pm W + v_\pm \Delta_{\hat{x}} W) = -\rho_\pm v_\pm W$$

and this yields

$$v''_\pm = \left(\Lambda_\pm^2 - \frac{\zeta_{\hat{\boldsymbol{\ell}},d}}{(\widetilde{\mathcal{L}})^2}\right) v_\pm = (\Gamma_\pm^{\hat{\boldsymbol{\ell}}})^2 v_\pm, \quad \Lambda_\pm^2 = \frac{\rho_\pm}{m_\pm} \quad \text{and} \quad \Gamma_\pm^{\hat{\boldsymbol{\ell}}} = \sqrt{\Lambda_\pm^2 - \frac{\zeta_{\hat{\boldsymbol{\ell}},d}}{(\widetilde{\mathcal{L}})^2}}.$$

We set

$$v_+(z) = a_+ \cosh(\Gamma_+^{\hat{\boldsymbol{\ell}}} z), \quad v_-(z) = a_- \cosh(\Gamma_-^{\hat{\boldsymbol{\ell}}}(\mathcal{L} - z)),$$

for some unknowns $a_+(t)$ and $a_-(t)$ to be determined and choose $Y = W$. Imposing the boundary conditions, we obtain

$$a_+(q^*) = \frac{1}{\cosh(\Gamma_+^{\hat{\boldsymbol{\ell}}} q^*)}\left(d_+\Lambda_+ \tanh(\Lambda_+ q^*) - \frac{\gamma\beta}{2}\frac{\zeta_{\hat{\boldsymbol{\ell}},d}}{(\widetilde{\mathcal{L}})^2}\right),$$

$$a_-(q^*) = -\frac{1}{\cosh(\Gamma_-^{\hat{\boldsymbol{\ell}}}(\mathcal{L}-q^*))}\left(d_-\Lambda_- \tanh(\Lambda_-(\mathcal{L} - q^*)) + \frac{\gamma\beta}{2}\frac{\zeta_{\hat{\boldsymbol{\ell}},d}}{(\widetilde{\mathcal{L}})^2}\right).$$

Meanwhile, we have

$$2\dot{Y} = \left(S_+ - S_- - m_+ a_+(q^*)\Gamma_+^{\hat{\boldsymbol{\ell}}} \sinh(\Gamma_+^{\hat{\boldsymbol{\ell}}} q^*) - m_- a_-(q^*)\Gamma_-^{\hat{\boldsymbol{\ell}}} \sinh(\Gamma_-^{\hat{\boldsymbol{\ell}}}(\mathcal{L} - q^*))\right) Y =: \alpha Y$$

with amplification factor α.

We consider parameters s.t. $\alpha > 0 \Rightarrow$ instabilities from interface perturbations.

We fix $\hat{\boldsymbol{\ell}} = (\ell_2, ..., \ell_d)$, and take

$$S_+ = -1, \quad S_- = m_\pm = \rho_\pm = 1, \quad d_+ = -1, \quad d_- = 1, \quad \Lambda_\pm = 1,$$

so that the stationary state is $q^* = \frac{\mathcal{L}}{2}$. Moreover $\Gamma_\pm^{\hat{\boldsymbol{\ell}}}$, $a_+(q^*)$ and $a_-(q^*)$ are explicit and

$$\alpha = -2 + \sqrt{1 + \frac{|\hat{\boldsymbol{\ell}}|^2\pi^2}{\widetilde{\mathcal{L}}^2}} \tanh\left(\frac{\mathcal{L}}{2}\sqrt{1 + \frac{|\hat{\boldsymbol{\ell}}|^2\pi^2}{\widetilde{\mathcal{L}}^2}}\right)\left(2\tanh\left(\frac{\mathcal{L}}{2}\right) - \gamma\beta\frac{|\hat{\boldsymbol{\ell}}|^2\pi^2}{\widetilde{\mathcal{L}}^2}\right).$$

Perturbation of Planar Solutions - Conclusion

From $2\dot{Y} = \alpha Y$ we draw the following conclusions:

- $\hat{\ell} = \hat{0}$: translational perturbations $w = q^* + \epsilon$, we see that the amplification factor becomes negative. Thus:

$$\boxed{\hat{\ell} = \hat{0} \quad \Rightarrow \quad \text{stability with respect to translational perturbations}}$$

- $|\hat{\ell}| > 0$: perturbations of the form $w = q^* + \epsilon \cos(\pi \ell_2 x_2 / \widetilde{\mathcal{L}}) + \ldots + \epsilon \cos(\pi \ell_d x_d / \widetilde{\mathcal{L}})$. We see that α is positive when $\beta < \beta_{\text{crit}}(\hat{\ell})$, where

$$\beta_{\text{crit}}(\hat{\ell}) = \frac{2}{\gamma} \frac{\widetilde{\mathcal{L}}^2}{|\hat{\ell}|^2 \pi^2} \left(\tanh\left(\frac{\mathcal{L}}{2}\right) - \frac{1}{\sqrt{1+|\hat{\ell}|^2\pi^2/\widetilde{\mathcal{L}}^2}\tanh\left(\frac{\mathcal{L}}{2}\sqrt{1+|\hat{\ell}|^2\pi^2/\widetilde{\mathcal{L}}^2}\right)} \right).$$

As $|\hat{\ell}|^2 = (\ell_2)^2 + \cdots + (\ell_d)^2$, we obtain that the possible perturbations lead to amplification factors via sum of squares. For $d = 2$ we obtain $|\hat{\ell}|^2 = 0, 1, 4, 9, \ldots$ and for $d = 3$ we have $|\hat{\ell}|^2 = 0, 1, 2, 4, 5, 8, 9, 10, \ldots$.

$$\boxed{|\hat{\ell}| > 0 \text{ and } \beta \text{ small} \quad \Rightarrow \quad \text{instabilities}}$$

Numerical results

Numerics - 2D

Figure 3: ($\varepsilon = \frac{1}{32\pi}$, $\Omega = (0,1)^2$) Evolution for $\beta = 0.1$, $S_- = 8$, $S_+ = -8$. We show the solution at times $t = 0, 0.1, 1, 2, 10$.

Figure 14: ($\varepsilon = \frac{1}{32\pi}$, $\Omega = (0,2)^2$) Evolution for $\beta = 0.002$, $S_- = 0.25$, $S_+ = -4$. We show the solution at times $t = 0, 0.2, 1, 2, 5$.

Figure 15: ($\varepsilon = \frac{1}{32\pi}$, $\Omega = (0,1)^2$) Evolution for $\beta = 0.002$, $S_- = 0.25$, $S_+ = -4$. We show the solution at times $t = 0, 0.2, 1, 2, 5$.

Numerics - 2D

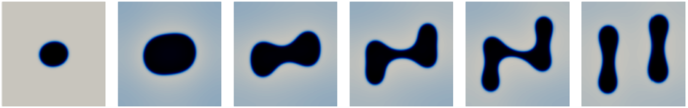

Figure 16: ($\varepsilon = \frac{1}{16\pi}$, $\Omega = (0,2)^2$) Evolution for $\beta = 0.02$, $S_- = 1$, $S_+ = -4$. We show the solution at times $t = 0, 2, 4, 6, 8, 10$.

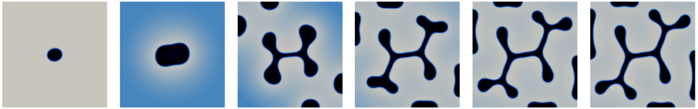

Figure 17: ($\varepsilon = \frac{1}{16\pi}$, $\Omega = (0,4)^2$) Evolution for $\beta = 0.02$, $S_- = 1$, $S_+ = -4$. We show the solution at times $t = 0, 2, 4, 6, 8, 10$.

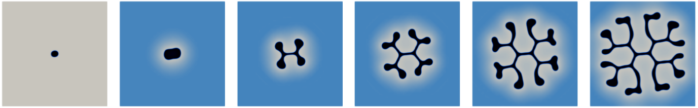

Figure 18: ($\varepsilon = \frac{1}{16\pi}$, $\Omega = (0,8)^2$) Evolution for $\beta = 0.02$, $S_- = 1$, $S_+ = -4$. We show the solution at times $t = 0, 2, 4, 6, 8, 10$.

Numerics - 3D

Figure 45: ($\Omega = (-4,4)^3$) perturbed data with $r_0 = 0.65$, $m_- = 0.1$, $m_+ = 7$, $\beta = 0.1$, $S_- = 1.4$, $S_+ = -7$, $\rho_- = 0.065$, $\rho_+ = 0.1$, $L = -1$. Below the solution at times $t = 0.5, 1, 1.5, 2$.

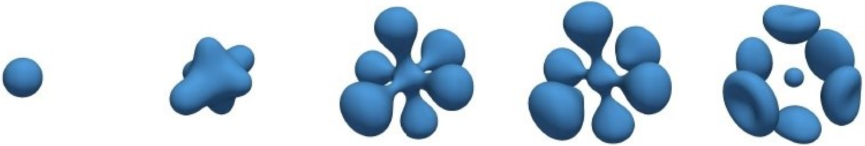

POLITECNICO
MILANO 1863

Conclusions:

We propose a **Cahn–Hilliard** model for **active droplets**, deriving a **sharp interface** model and performing stability analysis that identifies both stable and unstable solutions. **Numerical simulations** validate the theoretical findings.

Alexander von
HUMBOLDT
STIFTUNG

Recap (continues)

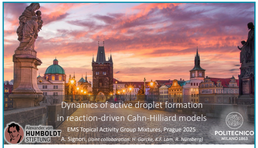

Slide 1

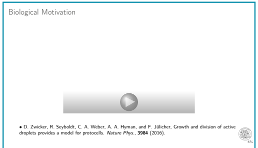

Slide 2

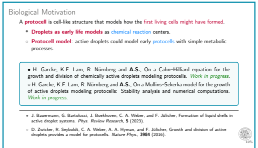

Slide 3

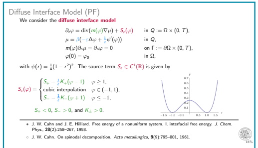

Slide 4

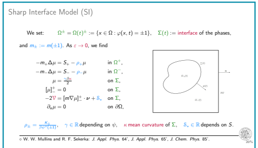

Slide 5

Slide 6

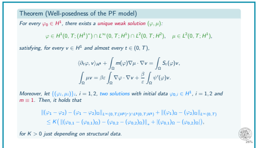

Slide 7

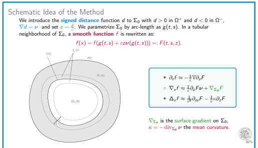

Slide 8

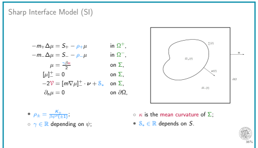

Slide 9

Slide 10

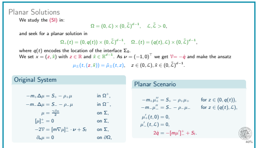

Slide 11

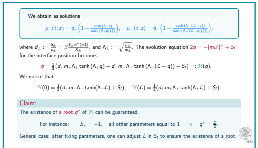

Slide 12

Recap (continues)

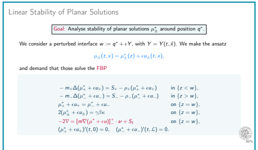

Slide 13

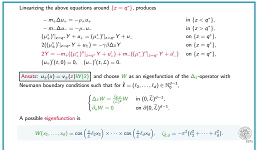

Slide 14

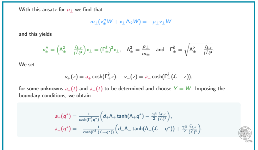

Slide 15

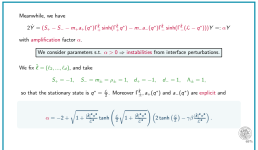

Slide 16

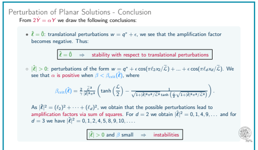

Slide 17

Slide 18

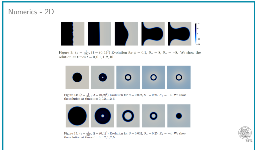

Slide 19

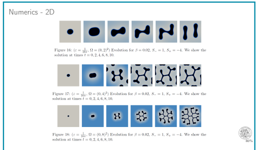

Slide 20

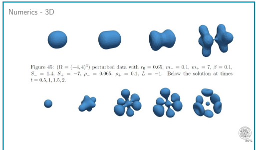

Slide 21

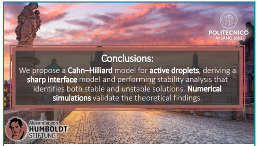

Slide 22